35th Annual International Conference of the IEEE EMBS
Osaka, Japan, 3 - 7 July, 2013

# A novel online recalibration strategy for continuous glucose measurement sensors employing LMI techniques

Harald Kirchsteiger, Luca Zaccarian, Eric Renard, and Luigi del Re

*Abstract*— **This paper considers the problem of online calibration and recalibration of continuous glucose monitoring devices. A parametric relation between interstitial and blood glucose is investigated and a constructive algorithm to adaptively estimate the parameters within this relation is proposed. The algorithm explicitly considers measurement uncertainty of the device used to collect the calibration measurements and enables automatic detection of measurements which are not suitable to be used for calibration. The method was assessed on clinical data from 17 diabetic patients and the improvements with respect to the current state of the art is shown.**

## I. Introduction

In the effective treatment of diabetes it is essential to measure the blood glucose concentration (BG) frequently throughout the day by self monitoring of BG (SMBG). Traditionally, this involves extraction of a small quantity of capillary blood from a finger which is applied on a disposable test strip. In contrast, continuous glucose monitoring (CGM) devices provide a continuous estimation of the current BG based on measurements in the interstitial fluid of subcutaneous (SC) tissues. However, the accuracy of CGM systems is not comparable with SMBG [1], and so far no CGM sensor was approved as a replacement of traditional monitoring devices [2]. In the particular situations of insulin dosage decision or administration of diabetes medication, traditional BG measurements must be performed [2]. Measuring BG is currently considered as a major limiting factor in the development of automated diabetes control systems [3].

Most of the available CGM devices measure an electrical current in the SC tissues proportional to the interstitial glucose concentration (IG), exploiting the glucose-oxidase enzyme reaction. To relate this measurement to the desired BG a calibration is necessary which is usually accomplished through an affine relation of the form $x = ay + b$ [4] where $x$ is the BG obtained through SMBG, $y$ is the measured current and $a, b$ are the calibration constants. Care has to be taken in choosing appropriate calibration measurements [5]: it is recommended to calibrate at times when the signals are mostly in a static rather than dynamic regime. Once the device is calibrated the calibration will get lost over time mainly because of a process called *Biofouling* [6] which, as protein molecules stick to the sensor element, continuously alters the diffusion process. Therefore, sensor needles need to be entirely replaced every 5-7 days and recalibration measurements are required every 12-24 hours [7].

The state of the art calibration technique described above does not take into account IG to BG dynamics well known from physiology, e.g. the time-lag between the two compartments of approximately 4-10 minutes [8]. In [9], a linear first order filter is assumed between the two compartments and the time-constant $\tau$ within this relation estimated continuously with the aid of an extended Kalman filter. A recently presented method [7] also proposes a first order filter model with an impulse response of the form $1/\tau \exp(-t/\tau)$ between the two compartments where $\tau$ is an a-priori fixed time constant. Superiority compared to state of the art methods was shown in simulation and on real data, however, the method might be further improved if $\tau$ could be adapted online.

Here, we propose such a model based adaptive method capable of solving the problem of calibration and online recalibration by assuming a pure time delay between the IG and BG compartments. The parameters are estimated online by solving convex optimization problems. The algorithm is of moderate computational complexity and could be implemented in a signal post-processing unit on CGM devices.

## II. Problem Statement

We address the problem of calibration of the signal produced by a sensor installed on a patient, which provides a continuous measurement signal $y_{int}(\cdot)$ related to the IG. Based on past results present in the literature [3], [4], [10], the raw measurement signal $y_{int}$ is a function of the actual glucose concentration $x_{int}$ in the interstitial fluid and can be described with the affine function:

$$x_{int}(t) = k_1 y_{int}(t) + k_0, \quad t \in \mathbb{R}, \tag{1}$$

where $k_0,\ k_1$ are the unknown calibration constants. In the sequel, we will denote $y_{int}$ as the *continuous measurements*. The typical approach which is followed in the literature [4] to estimate the pair $k_0,\ k_1$ is to rely on high accuracy sampled measurements $y_{blood}$ of the BG — measured directly using venous blood samples in clinical applications or by patients SMBG — which is strongly related to the IG [11], [12]. In particular, the current methods for measurement of BG are

This work was supported in part by the COMET K2 center "Austrian Center of Competence in Mechatronics (ACCM)". The COMET program is funded by the Austrian federal government, the federal state Upper Austria and the scientific partners of ACCM.

H. Kirchsteiger and L. del Re are with the Institute for Design and Control of Mechatronical Systems, Johannes Kepler University Linz, 4040 Linz, Austria harald.kirchsteiger@jku.at, luigi.delre@jku.at

L. Zaccarian is with the University of Trento and with the CNRS, LAAS, 7 avenue du colonel Roche, F-31400 Toulouse, France and Univ. de Toulouse, LAAS, F-31400 Toulouse, France zaccarian@laas.fr.

E. Renard is with the Department of Endocrinology, Diabetes and Nutrition and CIC INSERM 1001 at Montpellier University Hospital, France e-renard@chu-montpellier.fr

978-1-4577-0216-7/13/$26.00 ©2013 IEEE

$$\min_{T\in[0,T_{max}]} \epsilon(T) \triangleq \min_{k_0,k_1} \sum_{i\in\mathcal{I}(t)} \eta_i, \quad \text{subject to}: \eta_i \geq 0, \quad \forall i \in \mathcal{I}, \tag{6a}$$

$$\begin{bmatrix} \Delta(y_{blood}(t_i))^2 + \eta_i\psi(\bar{t}-t_i) & k_0 + k_1 y_{int}(t_i+T) - y_{blood}(t_i) \\ \star & 1 \end{bmatrix} \geq 0, \quad \forall i \in \mathcal{I} \tag{6b}$$

characterized by a reasonably small confidence range and can be characterized by the following relation:

$$x_{blood}(t_i) \in y_{blood}(t_i) + \mathcal{B}\left(\Delta(y_{blood}(t_i))\right), \quad i \in \mathbb{Z}, \tag{2}$$

where $t_i$ denote the times when the patient performs the measurement, $x_{blood}$ is the actual (unknown) BG, $\mathcal{B}(v)$ the interval $[-v, v]$ and $\Delta(\cdot)$ is a function characterizing the confidence level of the measurement. One typical characterization of $\Delta(\cdot)$ is a linear strictly increasing function (the smaller the measured value, the higher the confidence of the measurement is). In the sequel, we will denote $y_{blood}$ as *high precision* or *sampled measurements*.

Here, we will investigate the calibration problem by establishing a parametric relation between the BG and IG and, in addition to estimating the calibration constants $k_0,\ k_1$ in (1), we will also use $y_{int}(t)$, $t \in \mathbb{R}$, $y_{blood}(t_i)$, $i \in \mathbb{Z}$, to estimate the parameters within this relation. We focus on relating the two concentrations by a pure time delay, resembling the fact [8] that upon a sudden increase of the BG, the same increase is detected in the IG after a suitable delay:

$$\hat{x}_{blood}(t) = x_{int}(t+T). \tag{3}$$

where $T$ the delay to be estimated. Using (II), the BG can be estimated from the knowledge of the IG.

In the rest of the paper we will use convex optimization tools to address the following problem.

*Problem 1:* Given the continuous and high precision measurements in (1) and (2), respectively, and the linear model (II), for each time $t \in \mathbb{R}$, define the set of indices

$$\mathcal{I}(t) \triangleq \{i : t_i \leq t\}, \tag{4}$$

denote $\bar{t} \triangleq \max_{j\in\mathcal{I}} t_j$ and determine a solution to the following optimization problem

$$\begin{aligned} (k_0^*(t),\ k_1^*(t),\ T^*(t)) = \operatorname*{argmin}_{k_0,k_1,T} & \sum_{i\in\mathcal{I}(t)} \eta_i \\ \text{subject to}: \text{(II)}, \quad & \eta_i \geq 0,\ i \in \mathcal{I}(t) \\ & |\hat{x}_{blood}(t_i) - y_{blood}(t_i)|^2 \leq \Delta(y_{blood}(t_i))^2 \\ & + \eta_i\psi\left(\bar{t}-t_i\right), \quad i \in \mathcal{I}(t) \end{aligned} \tag{5}$$

where $\psi(\cdot)$ is a nondecreasing positive function representing a desired forgetting factor for the parameter estimates and $\eta_i$ are the optimization variables.

*Remark 1:* Note that a zero value of the cost, $\sum_{i\in\mathcal{I}(i)} \eta_i$, implies that all predicted and actual measurements are within the tolerance of the sampled measurements.

Note also that in problem (5) the optimization is carried out at time $t$ by only taking into account the past high precision measurements (this is embedded in the definition of $\mathcal{I}(t)$), therefore the optimization can be carried out in a causal way although, an additional delay of at least $T$ minutes is required, so that the signal $y_{int}(t+T)$ is available.

## III. Recalibration Strategy

*Proposition 1:* Given $t \in \mathbb{R}$, consider the index set (4). Assume that for some $T_{max} > 0$, the optimization problem (6) at the top of the page where $\star$ denotes a symmetric entry has a unique global optimum. Then the optimal values $(T^*, k_0^*, k_1^*)$ solve Problem 1 restricted to $T \in [0, T_{max}]$.

*Proof:* Using (3), the last constraint in (5) becomes

$$\begin{aligned} |k_0 + k_1 y_{int}(t_i+T) - y_{blood}(t_i)|^2 & \\ \leq \Delta(y_{blood}(t_i))^2 + \eta_i\psi(\bar{t}-t_i) & \end{aligned}$$

Using a Schur complement [13] this is equivalent to (6b). ■

Note that the inner optimization problem in (6) is a set of linear matrix inequalities in the unknown variables $\eta_i$, $i \in \mathcal{I}$ and $k_0, k_1$, which can be efficiently solved using standard tools [14]. Since the case studies that we will address are characterized by a device providing a sequence of values $y_{int}(t_k)$, $t_k = kT_s$, $\forall k \in \mathbb{Z}$, we illustrate in the following procedure a sensor calibration strategy exploiting Proposition 1 which addresses this special case.

*Procedure 1:*

**Step 1.** Fix a forgetting function $\psi(\cdot)$ and the maximum expected delay $T_{max}$. Fix $(k_0^*, k_1^*, T^*) = (0, 0, 0)$.

**Step 2.** Wait for the next high precision measurement $y_{blood}(t_{hp})$. Compute $\mathcal{I}(t_{hp})$. Wait for the next continuous measurement $y_{int}(t)$. Initialize $T = t - t_{hp}$ and compute the optimal value $\epsilon(T)$ of the inner convex optimization problem in (6). Set the initial and optimal values $\epsilon_0 = \epsilon^* = \epsilon(T)$. Initialize the state $\epsilon = \epsilon_0$.

**Step 3.** Wait for the next continuous measurement and, using the next state $T^+ = t - t_{hp}$, compute the optimal value $\epsilon^+ \triangleq \epsilon(T^+)$ of the inner convex optimization problem in (6) and denote by $(k_0, k_1)$ the optimal parameters.

**Step 4.** If $(\epsilon^+ - \epsilon)(\epsilon^+ - \epsilon^*) \leq 0$ then report an error and go back to step 2: the function $\epsilon(T)$ is not quasi-convex in $[0, T_{max}]$. Otherwise goto the next step.

**Step 5.** Shift forward $\epsilon = \epsilon^+$ and $T = T^+$. If $\epsilon \leq \epsilon^*$, then set $\epsilon^* = \epsilon$ and $(k_0^*, k_1^*, T^*) = (k_0, k_1, T)$.

**Step 6.** If $T \leq T_{max}$ and $(\epsilon - \epsilon^*)(\epsilon - \epsilon_0) \leq 0$, then goto step 3. Otherwise compute $e = \text{sign}((\epsilon_0 - \epsilon^*)(\epsilon - \epsilon^*))$. If $e = 0$, report an error: the function does not have a minimum in $[0, T_{max}]$. If $e > 0$, then update the calibration parameters with the optimal values $(k_0^*, k_1^*, T^*)$. Go to step 2 to wait for the next high-precision measurement.

The rationale behind Procedure 1 is illustrated in Fig 1: At time $t_{hp}$ a new high precision measurement is entered in the device. Then a sequence of optimizations are carried out as $y_{int}(t)$, $t \geq t_{hp}$ become available. Then, with reference to the top plot of Fig. 1, the sequence of optimal values $\epsilon(t_k - t_{hp})$ is expected to decrease until the optimal delay

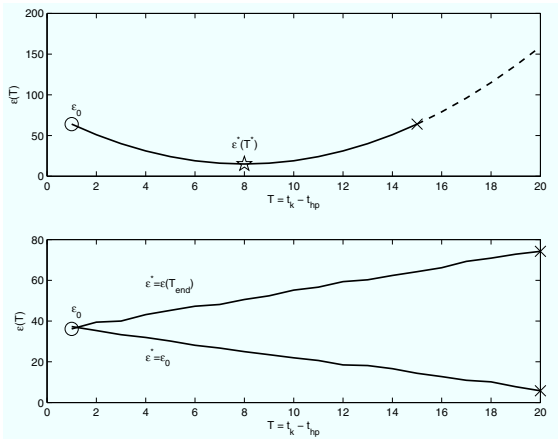


Fig. 1. Illustration of Procedure 1: Expected shape of $\epsilon(T)$, top panel; two abnormalities detected at Step 6 of the procedure, bottom panel.

$T^*$, is reached (this is marked by an "$\star$"). Subsequently, it is expected to increase and the algorithm terminates when the current value of $\epsilon$ is different from the current minimum $\epsilon^*$ and larger than the initial value $\epsilon_0$ (this is marked by an "$\times$"), or the maximum time $T_{max}$ is elapsed.

In normal operating conditions, the expected curve is "U"-shaped with a single minimum value $T \in [0, T_{max}]$. Whenever the detected function does not comply with these requirements, Procedure 1 terminates with a fault. In particular, if $\epsilon(T)$ is monotonically nonincreasing or nondecreasing, then the check at Step 6 results in $e = 0$ and the procedure returns a faulty result. Moreover, if the function has one or more local maxima in the interval, then the test at Step 4 will give a faulty result. If the procedure terminates with a fault, the calibration constants simply remain unchanged and the high precision measurement is disregarded.

## IV. Assessment on Experimental Data

### A. Description of the data set

In total, datasets coming from 17 patients consisting of 3 day in-hospital data collected at the Centre d' Investigation Clinique (CIC INSERM 1001) at Montpellier University Hospital, France have been used in this work. The continuous measurements have been collected with the FreeStyle Navigator™(Abbott Diabetes Care, Alameda, CA). The CGM data consists of a series of blood glucose concentrations, estimated every minute from the mean signal related to the glucose concentration in the SC interstitial fluid over this time period and calibrated against SMBG performed on a timely basis according to the manufacturer instructions. Additionally, the raw electrical current signal measured in the interstitial fluid and sampled on a one minute basis is available. High precision measurements were taken with a HemoCue $\beta$-glucose system (HemoCue AB, Angelholm, Sweden) at times 10, 20, 30, 45, 60, 90 and 120 min after a meal and at 2-hour intervals thereafter. Additionally, patients used their personal strip-based BG meter individually. Those measurements were typically performed before and some hours after each meal.

We test the proposed method on all datasets, by using all high-precision measurements until midnight of day 1 and roughly six measurements in the following days day for the calibration algorithm. To assess the quality of the calibration, all high-precision measurements are considered.

TABLE I

Average rel. errors

| Id | Day 3 | | | Overall | | | |
|---|---|---|---|---|---|---|---|
| | Smp | Delay | Sens | Fails | **Smp** | **Delay** | **Sens** |
| 1 | 27/6 | 7 | 21 | 6 | 97/45 | 7 | 18 |
| 2 | 29/6 | 12 | 12 | 8 | 102/46 | 11 | 11 |
| 3 | 27/6 | 9 | 15 | 18 | 104/45 | 9 | 10 |
| 4 | 30/5 | 13 | 12 | 2 | 105/43 | 10 | 13 |
| 5 | 29/6 | 7 | 9 | 7 | 100/47 | 7 | 10 |
| 6 | 36/6 | 15 | 26 | 11 | 111/49 | 11 | 20 |
| 7 | 27/7 | 5 | 16 | 4 | 98/48 | 8 | 15 |
| 8 | 27/7 | 7 | 10 | 5 | 108/54 | 9 | 14 |
| 9 | 7/3 | 10 | 13 | 6 | 62/39 | 7 | 11 |
| 11 | 28/6 | 7 | 14 | 2 | 98/44 | 6 | 12 |
| 15 | 27/6 | 10 | 15 | 15 | 97/45 | 7 | 9 |
| 16 | 3/4 | 10 | 15 | 3 | 64/41 | 8 | 12 |
| 18 | 30/9 | 13 | 16 | 2 | 111/55 | 13 | 17 |
| 19 | 28/6 | 5 | 14 | 4 | 99/46 | 5 | 12 |
| 20 | 26/7 | 11 | 16 | 10 | 96/49 | 9 | 16 |
| 28 | 20/6 | 9 | 23 | 7 | 71/36 | 7 | 20 |
| 30 | 21/6 | 8 | 10 | 15 | 77/38 | 17 | 19 |
| Net | 25/6 | 9 | 15 | 7 | 94/45 | 9 | 14 |

### B. Calibration results using the delay model

We follow Procedure 1 selecting $T_{max} = 30$ min., the forgetting function $\psi$ as the interpolation of the following data points (time in hours): $(\psi(0), \psi(1), \psi(2), \psi(4), \psi(6), \psi(12), \psi(24), \psi(48)) = (1, 3.5, 5, 6, 7, 9, 12, 20)$ and the tolerance level function $\Delta(v) = v/30$. Moreover, we limit the cardinality of the index set $\mathcal{I}$ in (4) to 10, as a larger number of measurements essentially does not make any difference due to the effect of the forgetting function. To assess the quality of the proposed calibration strategy, we consider all high-precision measurements and compare them to the expected glucose concentration determined by evaluating the model (II) where $T$ corresponds to the estimated optimal parameter.

Table I lists, for each patient, the rel. errors and the number of samples "Smp" used for assessment/calibration. Notice that all samples are used for calibration on day 1, while only a reduced number are used in the other days. The "Delay" and "Sens" columns report on the error using our model and the error of the CGM sensor output, respectively. The section "Overall" reports the same statistics over all 3 days and additionally indicating the number of failures reported by Procedure 1 in "Fails". Failures are generally expected and correspond to possibly inconsistent measurements and simply lead to leaving unchanged the calibration parameters.

From Table I it appears that the overall average error arising from the proposed calibration technique is never worse than the one obtained from the sensor output. In Fig. 2 and 3 we report the time histories for patient 19, which corresponds to the best performance of Table I and patient 30, which corresponds to the worst performance of Table I. In both figures, the upper plot reports the whole trace, where the blue diamonds represent the whole set of high precision measurements used for performance assessment, while the

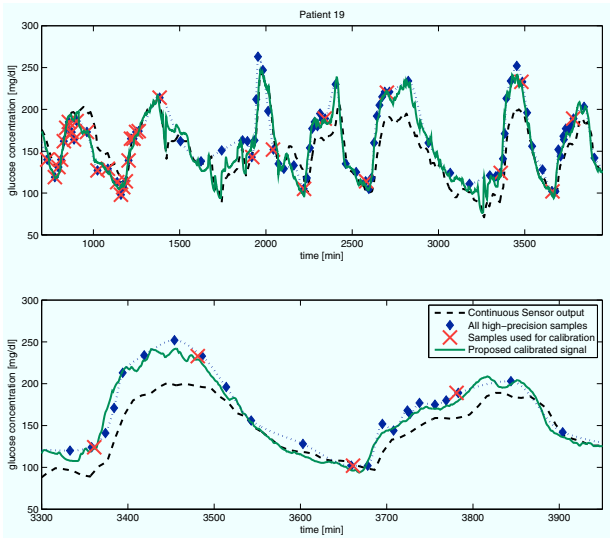


Fig. 2. Glucose levels for patient 19

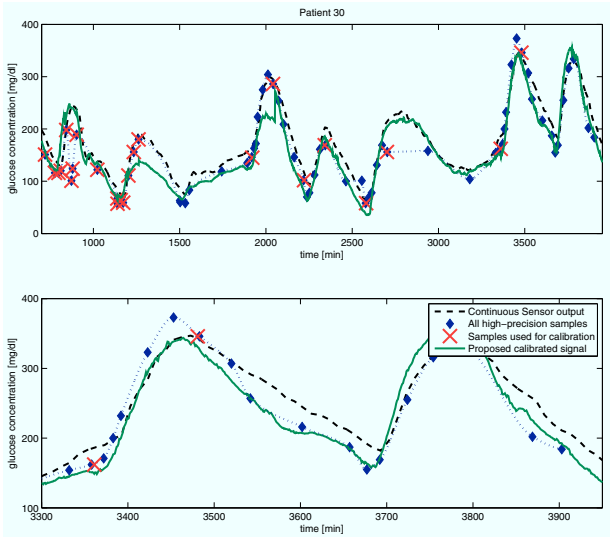


Fig. 3. Glucose levels for patient 30

red "X"s correspond to the ones used for calibration. The high-precision samples are also interpolated using a "pchip" fit, to provide a rough estimate of the actual BG. The black dashed trace is the sensor output, while the green solid trace is the calibrated signal arising from Procedure 1. In the lower plot of the two figures we show a zoomed portion of data corresponding to the last 700 minutes. The good fit provided by the model for patient 19 can be appreciated in Fig. 2 where the green solid trace always remains very close to the high-precision samples. As for patient 30 and the curves of Fig. 3, an interesting feature is that most of the errors come from inaccurate measurements for large values of the glucose concentration, whereas the accuracy for small glucose levels remains quite good.

## V. Conclusions

A strategy for on-line calibration of raw measurement signals from a CGM device was presented. It assumes an affine dependence of the electrical current measured in the interstitial fluid and the IG and a time-delay between the IG and BG compartment. As opposed to available results, the method can explicitly take into account a given measurement uncertainty of the device used to collect the calibration measurements. An efficient way to implement the procedure was presented. As a by-product, information on the reliability of the measurements may be obtained. This is a particularly appealing practical feature when considering that inappropriate calibration measurements deteriorate the signal performance. If the user provides such a measurement, it could be detected as inappropriate and neglected in the recalibration process. Validation of the algorithm on real measurement data coming from 17 patients was performed. The results showed that recalibrated signals are much closer to the actual BG even in the case when only few calibration measurements are performed and even when those measurements are performed from the patients themselves with their own devices.

## References

[1] B. Kovatchev, L. Heinemann, S. Anderson, and W. Clarke, "Comparison of the numerical and clinical accuracy of four continuous glucose monitors," *Diabetes Care*, vol. 31, no. 6, pp. 1160–1164, 2008.

[2] I. B. Hirsch, D. Armstrong, R. M. Bergenstal, B. Buckingham, B. Childs, W. L. Clarke, and A. Peters, "Clinical application of emerging sensor technologies in diabetes management: Consensus guidelines for continuous glucose monitoring (cgm)," *Diabetes Technology & Therapeutics*, vol. 10, no. 4, pp. 232–244, 2008.

[3] C. Cobelli, C. Dalla Man, G. Sparacino, L. Magni, G. De Nicolao, and B. P. Kovatchev, "Diabetes: Models, signals, and control," *IEEE Reviews in Biomedical Engineering*, vol. 2, pp. 54–96, 2009.

[4] V. Lodwig and L. Heinemann, "Continuous glucose monitoring with glucose sensors: calibration and assessment criteria." *Diabetes Technol Ther*, vol. 5, pp. 572–86, 2003.

[5] B. A. Buckingham, C. Kollman, R. W. Beck, A. Kalajian, R. Fiallo-Scharer, M. J. Tansey, L. A. Fox, D. M. Wilson, S. A. Weinzimer, K. J. Ruedy, and W. V. Tamborlane, "Evaluation of factors affecting cgms calibration," *Diabetes Technology & Therapeutics*, vol. 8, no. 3, pp. 318–325, 2006.

[6] U. Klueh, Z. Liu, B. Feldman, T. P. Henning, B. Cho, T. Ouyang, and D. Kreutzer, "Metabolic biofouling of glucose sensors in vivo: Role of tissue microhemorrhages," *Journal of Diabetes Science and Technology*, vol. 5, pp. 583–595, 2011.

[7] S. Guerra, A. Facchinetti, G. Sparacino, G. De Nicolao, and C. Cobelli, "Enhancing the accuracy of subcutaneous glucose sensors: A real-time deconvolution-based approach," *Biomedical Engineering, IEEE Transactions on*, vol. 59, no. 6, pp. 1658 –1669, june 2012.

[8] M. S. Boyne, D. M. Silver, J. Kaplan, and C. D. Saudek, "Timing of changes in interstitial and venous blood glucose measured with a continuous subcutaneous glucose sensor," *Diabetes*, vol. 52, no. 11, pp. 2790–2794, 2003.

[9] E. J. Knobbe and B. Buckingham, "The extended kalman filter for continuous glucose monitoring," *Diabetes Technology & Therapeutics*, vol. 7, no. 1, pp. 15–27, 2005.

[10] E. F. Pfeiffer, C. Meyerhoff, F. Bischof, F. S. Keck, and W. Kerner, "On line continuous monitoring of subcutaneous tissue glucose is feasible by combining portable glucosensor with microdialysis," *Horm Metab Res*, vol. 25, pp. 121–124, 1993.

[11] E. Kulcu, J. A. Tamada, G. Reach, R. O. Potts, and M. J. Lesho, "Physiological differences between interstitial glucose and blood glucose measured in human subjects," *Diabetes Care*, vol. 26, no. 8, pp. 2405–2419, August 2003.

[12] K. Rebrin, G. Steil, W. Van Antwerp, and J. Mastrototaro, "Subcutaneous glucose predicts plasma glucose independent of insulin: implications for continuous monitoring," *Am J of Physiology-Endocrinology and Metabolism*, vol. 277, no. 3, pp. E561–E571, Sep 1999.

[13] S. Boyd, L. E. Ghaoui, E. Feron, and V. Balakrishnan, *Linear Matrix Inequalities in System and Control Theory.* Society for Industrial and Applied Mathematics, 1994.

[14] P. Gahinet, A. Nemirovski, A. J. Laub, and M. Chilali, *LMI Control Toolbox.* The MathWorks Inc., 1995.